Paper I

Folkestad, A., Pettersson, L. H., and Durand, D. D. (2005)

Inter-comparison of ocean colour data products during algal blooms in the Skagerrak

Accepted for publication in
International Journal of Remote Sensing

Inter-comparison of ocean colour data products during algal blooms in the Skagerrak

A. FOLKESTAD[(1)], L. H. PETTERSSON[(1)], D. D. DURAND [(2)]

[(1)]Nansen Environmental and Remote Sensing Centre,
Thormøhlensgt 47, N-5006 Bergen, Norway
[(2)]Norwegian Institute for Water Research, Nordnesboder 5, N-5005 Bergen, Norway

Abstract
Several ocean colour (OC) Earth observation (EO) sensors are presently collecting data on an operational basis, including the Envisat MERIS sensor. This study aims at quantifying the differences in performance of the ocean colour EO sensors MERIS, MODIS/Aqua, and SeaWiFS for coastal monitoring and for the particular case of coastal algal bloom situations. The standard chlorophyll *a*, and radiance and reflectance products from the three sensors have been processed and compared for data acquired during the development of an early-spring algal bloom in 2004 in the eastern North Sea region. The study shows a high level of consistency between the Case 1 water Chl *a* products for all sensors. We conclude that the use of MERIS Chl *a* and other relevant products enable continued and possibly improved performance of an existing system for harmful algal bloom (HAB) detection and monitoring which up to December 2004 has been based on SeaWiFS.

Keywords: MERIS, MODIS, SeaWiFS, sensor comparison, algal blooms, North Sea

1. Introduction

The Nansen Environmental and Remote Sensing Centre (NERSC) has since 1998 established and operated a near real time (NRT) system for algal bloom monitoring in the North Sea Skagerrak region (Fig. 1). The system is based on NRT processing of Earth Observation (EO) data as well as information from discrete stations samples of *in situ* observations and numerical model outputs (Pettersson *et al.* 2000). The EO data sources provide estimates of the chlorophyll pigment concentration (Chl *a*), true colour surface reflections images (RGB), and sea surface temperature (SST). Until December 2004 data from the Sea-viewing Wide Field-of-View Sensor (SeaWiFS) (Hooker *et al.* 1992) was used as the prime EO data source. Since 2005 products from the Medium Resolution Imaging Spectrometer Instrument (MERIS) (Rast *et al.* 2000) onboard Envisat is used regularly. The EO and *in situ* observations are disseminated via the project website (http://HAB.nersc.no), and assessed in order to provide information about the algal bloom situation in Norwegian waters. Assessment reports are made in the case of detected bloom events and disseminated to key responsible authorities and industrial partners. In the event of harmful algal blooms (HABs) an early warning and subsequent predictions of the bloom evolution are essential for the national fishery authorities and for the fish farming industry in order to implement mitigation actions. The system therefore aims at early detection and subsequent monitoring of the spatial distribution of high-biomass algal bloom development and decay. Phytoplankton at low concentrations generates a weak optical signal from the ocean. To detect the presence of potential harmful phytoplankton

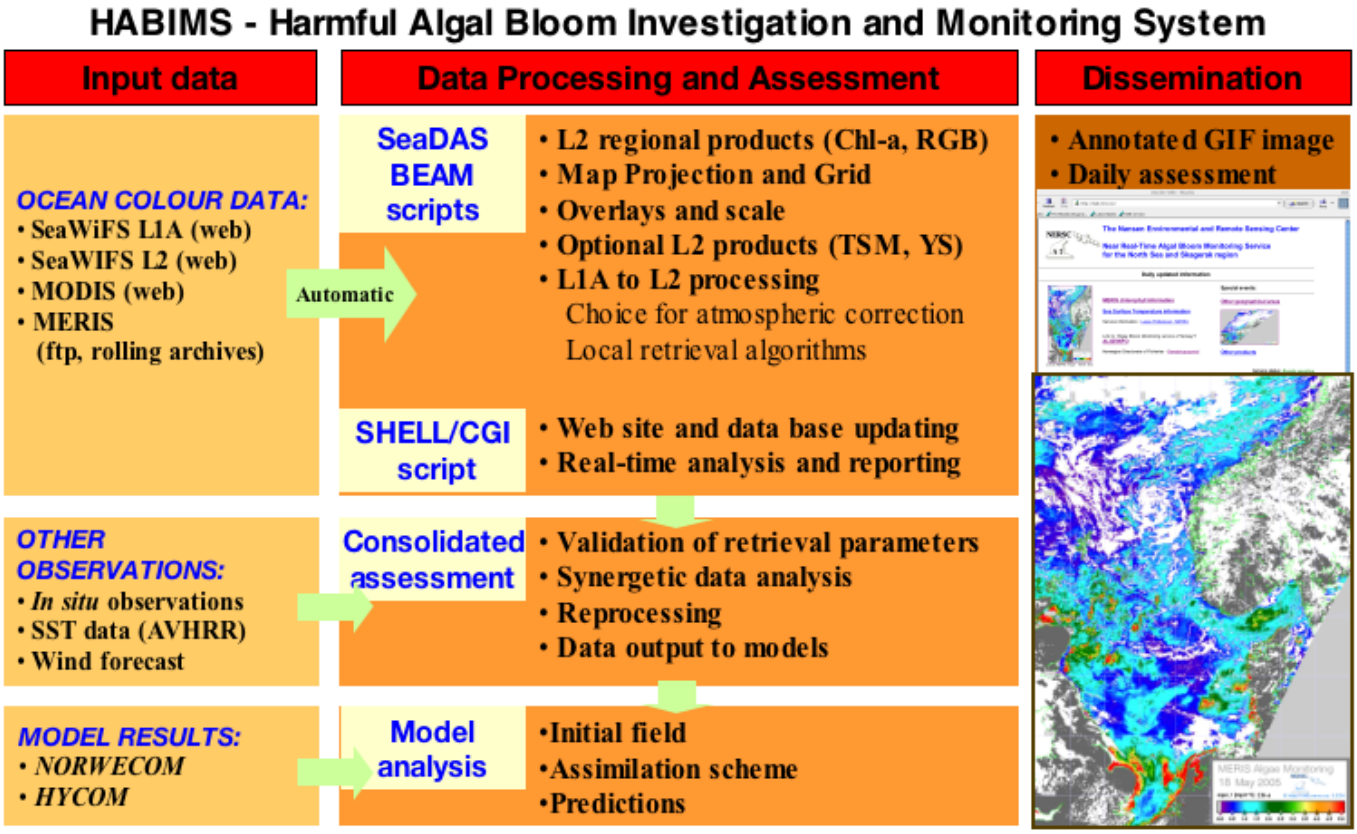

Figure 1: An overview of the Harmful Algal Bloom Investigation and Monitoring System (HABIMS) operated by NERSC. An integrated monitoring strategy is applied, in which data from various observation and modeling systems are used to assess information about the algal bloom situation in Norwegian waters. Daily updated information is disseminated via the project web site (http://HAB.nersc.no).

species at an early stage therefore requires high accuracy of the satellite biological and geophysical products. Moreover an integrated monitoring strategy (Fig. 1) is needed. Earlier major HAB events causing significant losses to aquaculture industry in Norway has been associated with high biomass flagellate blooms such as *Chrysocromulina polylepis* (Berge *et al.* 1989, Dundas *et al.* 1989, Johannessen *et al.* 1989) in 1988 and 1991 and *Chattonella* spp. (Horstmann *et al.* 1998, Durand *et al.* 2002) in 1998, 2000 and 2001. The EO-based sources are not capable of detecting whether a bloom is harmful or not, and accordingly *in situ* observations for bloom identification are crucial for the monitoring system. In the case of identified bloom events the satellite data are used to initiate and optimize dedicated field observations that are used to identify the bloom and eventually its species composition and possible harmfulness. The integrated set of observations is further used to improve the understanding of the (H)AB triggering and growth mechanisms.

After the launch of SeaWiFS several other ocean colour sensor systems have been put into orbit, providing an increased amount of EO data for determination of biological and physical marine information. Among these, MERIS onboard Envisat was launched in 2002, and the Moderate Resolution Imaging Spectroradiometer (MODIS) (Esaias *et al.* 1998) onboard Terra and Aqua satellites were launched in 1999 and 2002, respectively. However, these sensors have different technical design and specifications although they all are designed to provide similar estimates of Chl *a* in Case 1 waters. One of the concerns within the ocean colour research community is to develop methods to inter-calibrate sensors and data products so that consistent and long-term time series of ocean colour data products can be created independently of the specifications and lifetime of the individual sensor systems (Barnes *et al.* 2003). Also, by

merging information from several sensors, improved temporal resolution and coverage frequency can be obtained (Gregg *et al.* 1998). A number of studies have been conducted in order to map and evaluate the various sensor performances as well as inter-sensor differences with regards to the number of bands, their wavelength position and bandwidths of the spectral channels of each radiometer; the orbit configurations; the calibration and validation schemes; the atmospheric correction; and finally retrieval algorithms used(e.g. Gordon and Wang 1994, O'Reilly *et al.* 1998, Antoine and Morel 1999, Doerffer *et al.* 1999, Aiken and Moore 2000, Antoine and Morel 2000, Hu *et al.* 2000, Morel and Antoine 2000, O'Reilly *et al.* 2000, Siegel *et al.* 2000, Fournier-Sicre and Belanger 2002, Lee and Carder 2002, Blondeau-Patissier *et al.* 2004, Darecki and Stramski 2004, Gower and Borstad 2004, Zibordi *et al.* 2004).

One objective of the present study is to explore how routine products from new ocean colour sensors can contribute to improve the NRT early warning and monitoring of potential HABs in Norwegian coastal waters. Accordingly, the present study undertakes and inter-comparison of the three sensors (MERIS, MODIS/Aqua, and SeaWiFS) in order to evaluate the consistency between the sensor products, and subsequently to detect to what degree the performance of the monitoring system depends on which sensor is used. For the users of the monitoring system it is essential that regular and consistent information is made available whatever EO data source is used. Currently the detection and monitoring system uses the standard MERIS Chl *a* product designed for clear, oceanic (Case 1) waters. The sensor comparison is therefore based on equivalent products from the three ocean colour sensors, namely the standard Case 1 products for Chl *a* retrieval. The spectral surface reflectance (MERIS) and the normalized water-leaving radiance (MODIS and SeaWiFS) are also inter-compared between the sensors, since the Chl *a* products are derived from these measured optical quantities. This study does not intend to perform an absolute sensor validation or inter-calibration, but rather to carry out a sensor comparison and characterization, for practical use of the data products.

The second goal of this study is to evaluate a new method for detecting algal blooms and avoiding false alarms, i.e. situations where satellite retrievals indicate erroneously high pigment concentrations that subsequently are identified as possible bloom events. In Case 2 waters the standard Case 1 Chl *a* products are not generated with the accuracy needed for early detection of potential high biomass algal blooms. It has previously been shown that both the MODIS and SeaWiFS Case 1 water algorithms tend to overestimate Chl *a* in other European Case 2 waters, e.g. in the Baltic Sea (Darecki and Stramski, 2004) and in the southern North Sea (Blondeau-Patissier *et al.* 2004). A shortcoming of the Case 1 water algorithms for Chl *a* retrievals, and hence of the present algal bloom detection system, is the uncertainty in the ability to fully distinguish between Chl *a* and other optically active components (OACs) in the water column, such as suspended matter (SM) and yellow substance (YS). Major parts of the study area are frequently classified as Case 2 waters, introducing the possibility of false identifications of algal blooms if standard Case 1 products are used. To overcome this problem, new methods that better distinguishes between Chl *a* and other OACs must be used. The MERIS Case 2 water Chl *a* product is therefore evaluated. This product is developed to estimate Chl *a* in the waters where Chl *a* is not the only OAC present. In this study, this product's performance is compared to the three sensors' standard Case 1 water Chl *a* products, as well as briefly to *in situ* Chl *a* measurements. It is to be noticed that for the satellite dataset used in this study MERIS is the only sensor system providing an operational NRT Case 2 Chl *a* product. The MERIS Total Suspended Matter (TSM) and Yellow Substance (YS) products are also briefly investigated.

2. Data and Methods

2.1 Biological and hydrodynamical features in the study area

The study area covers the North Sea, Skagerrak, Kattegat, and the southern part of the Norwegian Coastal Current (NCC) (Fig. 2). Due to a complex

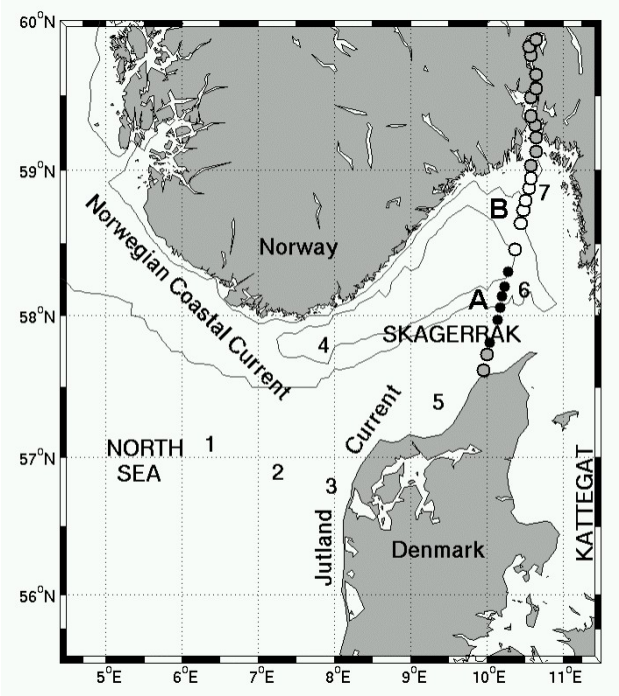

Figure 2: Map of study area. Iso-baths for 200m and 400m depth are shown. The numbers indicate the fixed locations for inter-comparison of satellite ocean colour products used in this study. The sampling points for *in situ* Chl *a* determination along the 'Color Festival' ferry transect between Oslo (Norway) and Hirtshals (Denmark) are indicated bydots and circles. Black dots and open (white) circles indicate sampling stations in region A and B, respectively (Table 3).

and variable circulation pattern of the water masses in this region, several sub-areas with distinct optical complexity are present. Generally, the central part of the North Sea is oligotrophic with low concentration of phytoplankton and optically "clear" waters. Due to sediment re-suspensions and river discharges the waters along the western coast of Denmark (the Jutland Current) are often loaded with sediments. Nutrient-rich terrigeneous and resuspended bottom waters from Continental Europe are transported northwards, causing favourable conditions for algal bloomsduring Spring and making the water optically complex due to the high loads of sediments and phytoplankton. In central parts of Skagerrak, between Norway and Denmark, the Jutland current mixes with the water from central North Sea, and the less saline

Table 1: The MERIS, MODIS/Aqua, and SeaWiFS sensors overpass time (UTC) for the 13 dates included in the studied dataset. All dates are in 2004.

	UTC		
Date	MERIS	MODIS/Aqua	SeaWiFS
Feb 18	10:43	12:35	12:31
Feb 21	10:49	11:25	12:55
Feb 23	09:45	11:15	12:37
Feb 24	10:54	11:55	11:39
Feb 29	09:56	12:15	13:24
Mar 03	10:01	12:45	12:09
Mar 08	10:44	11:25	12:15
Mar 09	10:12	12:10	12:56
Mar 18	10:28	12:05	12:27
Mar 25	10:07	12:10	12:16
Mar 30	10:54	12:25	12:22
Mar 31	10:21	11:35	13:03
Apr 01	09:52	12:15	12:05

outflow from the Baltic Sea through Kattegat. In the inner part of Skagerrak the waters are also influenced by coloured dissolved organic matter from river run-off primarily by the Glomma River, Norway. The NCC generally follows the Norwegian trench from central Skagerrak westwards and northwards along the Norwegian west coast (Sæthre and Mork 1981).

2.2 Ocean colour Earth Observation data

In this study data from the ocean colour sensors MERIS, MODIS/Aqua, and SeaWiFS were acquired for cloud free conditions in the study area during the period from February 18 to April 1, 2004. Within this period, 13 days of high quality data were identified for all the three sensors, for which the images were cloud free in major parts of the area of interest (Table 1). Due to different orbit configurations the three satellites have different local overpass time, accordingly the maximum differences in time between the three satellite passes was up to 3.5 hours. During the study period two distinct phytoplankton blooms were observed. Neither was in concentrations harmful to the environment as

Table 2: Specifications of the spectral bands of MERIS, MODIS and SeaWiFS sensors relevant for the bio-optics.

MERIS	MERIS band #	1	2	3	4	5	6	7
	Band centre (nm)	412.5	442.5	490	510	560	620	665
	Bandwidth (nm)	10	10	10	10	10	10	10
MODIS	MODIS band #	8	9	10	11	12		13
	Band centre (nm)	412	443	488	531	551		667
	Bandwidth (nm)	15	10	10	10	10		10
SeaWiFS	SeaWiFS band #	1	2	3	4	5		6
	Band centre (nm)	412	443	490	510	555		670
	Bandwidth (nm)	20	20	20	20	20		20

confirmed by species identification and phytoplankton cell counts from water samples.

2.2.1 MERIS data

For the present study processed MERIS Reduced Resolution (RR) Level 2 (L2) data were provided by the ESA ground segment processor using the latest revised algorithm for atmospheric correction at the time of acquisition and made available for calibration and validation purposes by ESA through Brockmann Consult, Germany. Information about the data and the processing is given in MERIS Cyclic Reports Cycle #24 and Cycle #25 (http://earth.esa.int/pcs/envisat/meris/reports/cyclic/) covering MERIS data acquired and processed during the time period from February 2 to April 12, 2004. Further data analyses and image generation were performed using the BEAM freeware from ESA (Basic ERS & Envisat (A)ATSR and Meris Toolbox (BEAM), version 2.3). A large number of geophysical (Level 2) ocean products are generated through the MERIS processing chain. We focused on algal pigment index 1 and 2 products (hereafter referred to as Algal 1 and Algal 2) that are equivalent to Chl *a* in Case 1 and 2 waters respectively, and the surface reflectance in MERIS bands 1-7 (Table 2).

Radiometric characteristics and the calibration of MERIS are defined in terms of reflectances. Radiances measured by the sensor at the top of the atmosphere (TOA) are converted to reflectances. In the MERIS Product Handbook (issue 1.2, September 2004, available at http://envisat.esa.int/dataproducts/meris/) the dimensionless water-leaving or surface reflectance, ρ_w, obtained after removing atmospheric contributions to the reflectance at TOA, is given as

$$\rho_w(\lambda) = \frac{\pi \cdot L_w(\lambda)}{E_d(\lambda)} \quad (1)$$

where $L_w(\lambda)$ is the upward directed water-leaving radiance at wavelength λ, and $E_d(\lambda)$ is the downwelling irradiance measured just above the water surface. The surface reflectance is not normalized to sun zenith or to nadir viewing angle. The Algal 1 product is derived from the ratio of $\rho_w(\lambda)$ at two wavelengths according to the following equation (Morel and Antoine, 2000):

$$\log_{10}(\text{Algal 1}) = \sum_{x=0}^{n} A_i (\log_{10} \rho)^x \quad (2)$$

where $\rho = \rho_w(443)/\rho_w(555)$, A_i are constant coefficients, and n denotes the order of expansion of the polynomial expression. According to the MERIS Product Handbook the Algal 2 product is given as

$$\text{Algal 2} = k_1 \left[a_{pig}(442) \right]^{k_2} \quad (3)$$

where $a_{pig}(442)$ (m^{-1}) is the pigment absorption at wavelength 442 nm. The factors of this scaling equation are given as k_1=26.212mg·m^{-2} and k_2=0.77135, but may be adjusted to local conditions. Detailed descriptions of the algorithms for atmospheric correction and the retrieval of the Algal 1 and Algal 2 products are presented in the MERIS Product Handbook and in (Antoine and Morel 1999, Moore *et al.* 1999, Aiken and Moore 2000, Antoine and Morel 2000, Morel and Antoine 2000).

2.2.2 MODIS/Aqua data

MODIS/Aqua L2 data were obtained from the NASA Ocean Color Discipline Processing System (OCDPS) at http://oceancolor.gsfc.nasa.gov/. The standard MODIS L2 ocean product suite includes normalized water-leaving radiances in 6 bands (Table 2), and Chl *a* in Case 1 waters retrieved by the OC3M algorithm (O'Reilly *et al*. 2000). The normalized water-leaving radiance provided by MODIS can be expressed as

$$\left[L_w(\lambda)\right]_N = \frac{L_w(\lambda)}{\mu_0 t_0(\lambda)} \quad , \qquad (4)$$

where $L_w(\lambda)$ is the water-leaving radiance, $t_0(\lambda)$ is the atmospheric diffuse transmittance in the solar direction, and μ_0 is the cosine of the solar zenith angle (e.g. Siegel *et al.* 2000). The normalized water-leaving radiance can be related to the water-leaving reflectance, $\rho_w(\lambda)$, through the equation

$$\rho_w(\lambda) = \frac{\pi\left[L_w(\lambda)\right]_N t_0(\lambda)}{F_0(\lambda)} , \qquad (5)$$

where $F_0(\lambda)$ is the extraterrestrial solar irradiance (Siegel *et al.* 2000). For convenience, the normalized water-leaving radiance will hereafter be denoted nLw.

The empirical OC3M algorithm used for retrieval of Chl *a* makes use of the remote sensing reflectance, $Rrs(\lambda)$, defined as the upwelling radiance leaving the water surface, $L_u(\lambda)$, normalized by the downwelling irradiance $E_d(\lambda)$, just above the water surface. The OC3M algorithm (O'Reilly *et al.* 2000) calculates Chl *a* as

$$\log_{10}(\text{Chl } a) = A_1 + A_2 R + A_3 R^2 + A_4 R^3 + A_5 R^4 \qquad (6)$$

where R is the $\log_{10}$ of the maximum band ratio:

$$R = \log_{10}\left\{\max\begin{bmatrix} Rrs(443)/Rrs(550), \\ Rrs(488)/Rrs(550) \end{bmatrix}\right\} \qquad (7)$$

and the coefficients A_1= 0.2830; A_2= -2.753; A_3= 1.457; A_4= 0.659; and A_5 = -1.403.

2.2.3 SeaWiFS data

SeaWiFS Local Area Coverage Level 1b data were retrieved from the NASA GSFC Distributed Active Archive Center (DAAC) together with ancillary meteorological and ozone data. The data were processed using SeaDAS v4.4. Atmospheric correction included multi-scattering, 765/865 model selection and NIR correction for non-zero nLw (Gordon and Wang 1994, Siegel *et al.* 2000). For the first six bands (Table2) nLw was retrieved. The standard OC4v4 algorithm (O'Reilly *et al.* 1998, O'Reilly *et al.* 2000) was used to retrieve Chl *a* in Case 1 waters. This algorithm is similar to the OC3M algorithm developed for MODIS bands, and calculates Chl *a* according to Eq. 6. However, the SeaWiFS wavelength band configuration enables the OC4v4 algorithm to select the maximum band ratio from three ratios as opposed to the two ratios in the OC3M algorithm. Therefore, in the OC4v4 algorithm R is given as

$$R = \log_{10}\left\{\max\begin{bmatrix} Rrs(443)/Rrs(555), \\ Rrs(490)/Rrs(555), \\ Rrs(510)/Rrs(555) \end{bmatrix}\right\} \qquad (8)$$

and A_1= 0.366; A_2= -3.067; A_3= 1.930; A_4= 0.649; and A_5 = -1.532. Equations 7 and 8 make it obvious that the different wavelength band configurations between MODIS and SeaWiFS may introduce discrepancies between their Chl *a* products.

2.3 Ground truth data

Water samples for determinations of *in situ* Chl *a* were collected by the ferrybox system operated by the Norwegian Institute of Water Research (NIVA) onboard the passenger ferry 'Color Festival' cruising twice a day between Oslo, Norway, and Hirtshals, Denmark. The sampling points along the ferry transect is indicated in Fig 2. The Chl *a* were determined with HPLC method according to the MERIS validation protocols (Doerffer, 2002).

The AlgeInfo web page (http://algeinfo.imr.no) provides weekly updated information on the algal situation in Norwegian

coastal waters, based on analyses of water samples from 27 coastal locations. Updated information about the abundance of phytoplankton and species composition of the phytoplankton community is given. Most information is based on near shore sampling. Information on the algal situation from the time period covering the ocean colour datasets was obtained from AlgeInfo. The phytoplankton abundance was given as cell counts and was as such not fulfilling the criteria for a proper validation of ocean colour data products. However, the cell counts provide indicative values of Chl *a*.

2.4 Methods of comparison

Data from the three EO sensors were inter-compared with regards to the spatial distribution patterns of Chl *a*, spatial frequency distributions of Chl *a*, spatial averaged values of Chl *a* over small areas at fixed locations, spatial averaged values of Chl *a* over larger homogeneous areas, as well as surface reflectance and normalized water-leaving radiance spectra at selected locations.

The data products were presented in the same projections and visualized for all 13 dates. Images from three dates are shown (Fig. 3). Visualization of the data in such a way enabled an overview of both the Chl *a* distribution patterns, the general consistency between the sensors' datasets and the smoothness of the retrieved signal for the different sensors. The results are presented and discussed in section 3.2.

For the studied dataset the frequency distribution of Chl *a* within each image was calculated and compared between the sensors. The Chl *a* data were grouped by concentration in 20 bins, each extending $1 mg \cdot m^{-3}$. For dates with significant differences between the cloud or swath coverage it was necessary to limit the comparison to sub-regions of the image, in order to exclude regions where data were lacking for any of the three sensors. Results from three dates (February 23, March 9, and April 1, 2004) are shown (Fig. 4) and discussed in section 3.2.

Within the study area seven fixed locations were defined for more in depth sensor comparison (Fig 1). These locations were intended to represent areas of water masses with different optical and biological properties. For the studied dataset Chl *a* values were calculated for each of these seven locations, enabling a sensor inter-comparison of Chl *a* for the various locations, as well as a study of the time evolution of Chl *a* for all locations. To reduce the impact of noise in the data, the Chl *a* values were compared between sensors as averages over the 5x5 pixel bins around these fixed locations, rather than as single pixel values. In the following, the seven boxes each containing 25 pixels are referred to as the "small areas". Substantial variability between neighbouring pixels was sometimes observed, especially for SeaWiFS, the reason of which is discussed in section 3.2. The dataset for comparison of Chl *a* in the small areas thus included up to 91 values for each sensor. However, for each sensor only data points where all pixels within the 5×5 pixel binning areas were processed and positive, contributed to the comparison and correlation analysis presented and discussed in section 3.3. The number of data values for inter-sensor comparison was therefore varying between 35 and 41 for the different sensors (Table 4). Avoiding negative pixels also reduces the impact of striping, which is sometimes evident in the MODIS/Aqua data (e.g. on February 23, Fig. 2). However, the striping effect may still influence the comparison between MODIS/Aqua and the other sensors, as this effect not necessarily generates negative pixel values.

Further, one to three larger areas depicting homogeneous Chl *a* were identified within the datasets for each of the 13 dates. These are in the following referred to as the "large areas". For each sensor, pixel values of Chl *a* were extracted from these large areas. The criteria for selecting the areas were (1) that they should be as large as possible but still be homogenous for all three sensors (with standard deviation of Chl *a* less than 30% of mean value), and (2) that eventual multiple areas from the same date should represent areas of different level of Chl *a* (i.e. within the low, medium or high concentration ranges). Following this procedure, within the studied dataset a total of 28 areas were selected for analysis. The inter-sensor comparison of the large areas therefore consisted of 28 data values. Due to differences in swath configurations, the

number of pixels within one area could vary between sensors. However, the number of pixels was generally in the order of 100 – ranging from 56 to 1950 for each homogeneous area compared between the three sensors. For each given area the mean values of Chl *a* were calculated for each sensor. The criterion for homogeneous areas (#1 above) prevented obvious strong Chl *a* gradients caused by e.g. fronts between water masses, eddies etc. to be present within any averaged areas.The spatial averaging of these data should therefore minimize the effect of oceanic dynamic effects from movements of fronts or eddies during the time differences between the overpasses of the three sensors (<3.5hrs). Because of the "large size" of the areas (as opposed to the small areas as described above), the results are expected to be less sensitive to differences in the pixel-by-pixel processing and the data quality. Results from this method of comparison are presented and discussed in section 3.4.

For MODIS/Aqua and SeaWiFS nLw in six overlapping bands (Table 2) were compared. For MERIS the standard product is the surface reflectance, which was studied for the first seven bands (Table 2). For the image from April 1, pixel values of these quantities were extracted for each sensor within a 5×5 pixel area around seven selected locations. Due to differences in the definition of the water-leaving signal between MERIS and the two US sensors (see sections 2.2.1-2.2.3), as well as the wavelength band configurations (see Table 2), a direct comparison of the products from the three sensors was not feasible. The spectral values of the MERIS surface reflectance were also important for identifying variations of optical properties between the selected locations, and for evaluating the quality of the atmospheric correction procedure (e.g. whether the retrieved reflectance values in the blue range of the spectrum is positive or not). Results from the comparison of normalized water-leaving radiances and surface reflectances are presented in section 3.5.

3. Results and Discussion

3.1 In situ observations

Between February 23 and 29, 2004, a massive algal bloom of *Skeletonema costatum* occurred in Skagerrak. Observed concentrations at the coastal sampling stations were 6 $\cdot 10^6$ cells/l (*AlgeInfo*, March 19, 2004). This bloom decayed rather quickly and was followed by a moderate concentration bloom (1.5 to 3 $\cdot 10^5$ cells/l) of the harmful species *Chattonella* spp. during the period of March 8-14. However, this bloom was at significantly lower concentrations than during previous events that had high negative impact on the environment (Pettersson *et al.* 2005). In the last week of March and the early days of April, only low algae abundance was reported (*AlgeInfo*, April 2, 2004).

Shipborne observations of Chl *a* obtained from the ferrybox system are summarized in

Table 3: Summary of ship borne (ferrybox system) observations of Chl *a* along a ship transect in the Skagerrak (Fig. 2). Data were available for three dates, for which minimum and maximum ferrybox Chl *a* observations are shown for two regions of the transect. Region A and B cover the southern and northern part of the transect respectively (Fig. 2). Each region contains six sampling stations where the retrievals of satellite and ship borne Chl *a* are compared. The average percentage retrieval error over the six stations is presented for the various sensors and algorithms.

Sampling date		Region	Ferrybox Chl *a*		Average retrieval error			
Ferrybox	Satellite		min [mg·m^{-3}]	max [mg·m^{-3}]	Alg2 [%]	Alg1 [%]	MOD [%]	Sea [%]
Feb 24	Feb 23	A	0.45	2.57	1025	167	87	89
Feb 24	Feb 23	B	3.61	6.01	253	79	73	109
Mar 09	Mar 09	A	4.29	6.70	16	-78	-36	-5
Mar 09	Mar 09	B	1.77	3.99	9	-69	-14	-3
Mar 30	Apr 01	A	0.43	1.03	89	185	202	153
Mar 30	Apr 01	B	0.46	2.71	150	139	291	161

Table 3. Along the ship transect two regions are defined, covering the southern (A) and northern (B) part of the transect. These regions are selected away from the coastline in order to avoid the adjacency effect in the satellite data. Within each region there are six sampling stations. Because of the general circulation pattern in the Skagerrak Chl *a* can be expected to be different between A and B. On February 24 the ship borne data reveal low or moderate Chl *a* in the south and high concentrations in the north. This is consistent with the presence of the *Skeletonema costatum* bloom along the Norwegian coast as reported by *AlgeInfo*. An inverse picture is observed on March 9 with high concentrations in the south and moderate in the north. This is not in contradiction to the reports of *Chattonella* present at the Norwegian coast since this bloom was also observed to be at moderate concentrations. On March 30 low or moderate Chl *a* are observed along the whole transect, also in consistency with the *Algeinfo* report.

3.2 Comparison of Chl a distribution patterns

The spatial distribution of Chl *a* in the study area was analyzed for the entire dataset. The three dates for which these results are shown (Fig. 3) were selected to illustrate the main features observed when comparing the data from the three sensors, and also represent different stages of the phytoplankton bloom. The images from February 23 (disregarding the Algal 2 product) resolve a similar pattern for the main Chl *a* distribution for all three sensors (Fig. 3). The bloom reported by *in situ* measurements along the Norwegian Skagerrak coast (Sørlandskysten) is clearly visible in the satellite images. High concentrations are also present in Kattegat between Denmark and Sweden. MERIS shows slightly higher concentrations along the Norwegian coast than the two other sensors. The Chl *a* retrieved by MERIS Algal 1 in central Skagerrak is around 2mg·m^{-3} or twice the values retrieved by MODIS/Aqua and SeaWiFS. However, all sensors tends to overestimate Chl *a* by a factor of at least two as compared to *in situ* measurements of February 24 (i.e. one day later) (Table 3). For the three dates from which the Chl *a* distributions are shown (Fig. 3), the frequency distributions of the retrieved Chl *a* from all sensors are shown in Fig. 4. Due to differences in swath and cloud cover contamination between images from the three sensors, only data from selected sub-regions of the original images (Fig. 3) were used for estimating the frequency distribution (see section 2.4). The frequency distribution of Chl *a* shows that for February 23 the number of pixels with Chl *a* values between 0 and 1mg·m^{-3} is 4-5 times less for MERIS Algal 1 than for MODIS/Aqua and SeaWiFS (Fig. 4a). Furthermore the number of pixels with Chl *a* values between 4 and 8 mg·m^{-3} is 2-5 times higher for MERIS Algal 1 than for the other sensors. This is mainly due to the higher MERIS Algal 1 values retrieved off western Jutland. However, a very good agreement between SeaWiFS and MODIS/Aqua Chl *a* values is observed. The MODIS/Aqua image is contaminated by stripes that most probably are originated from failure to correct for the sensor's radiometric response during calibration (e.g. as previously pointed out by Feldman and McClain, 2005b).

For March 9, the agreement between MODIS/Aqua and SeaWiFS is still very good, while MERIS Algal 1 shows generally lower values along the Norwegian Skagerrak coast (Figs. 3 and 4b). Both MODIS/Aqua and SeaWiFS retrieve high Chl *a* values (>3mg·m^{-3}) in central Skagerrak. For this date the MERIS data were flagged as Case 2 water in large parts of the area. Using the MERIS Algal 2 product, which should be more adequate for this type of water, an improved agreement between MERIS and the two other sensors for some areas including the ferry transect between Norway and Denmark is observed. Furthermore, both MODIS/Aqua Chl *a*, SeaWiFS Chl *a*, and the MERIS Algal 2 product gave values of Chl *a* close to the *in situ* measurements obtained the same day (Table 3).

The images from April 1 (Figs. 3 and 4c) show generally good agreement in the Chl *a* between all three sensors. However, due to atmospheric contamination around the southern part of Norway, the number of unprocessed pixels for both MERIS and SeaWiFS are rather high. Increased levels of Chl *a* (>5mg·m^{-3}) are again observed along the Norwegian Skagerrak coast

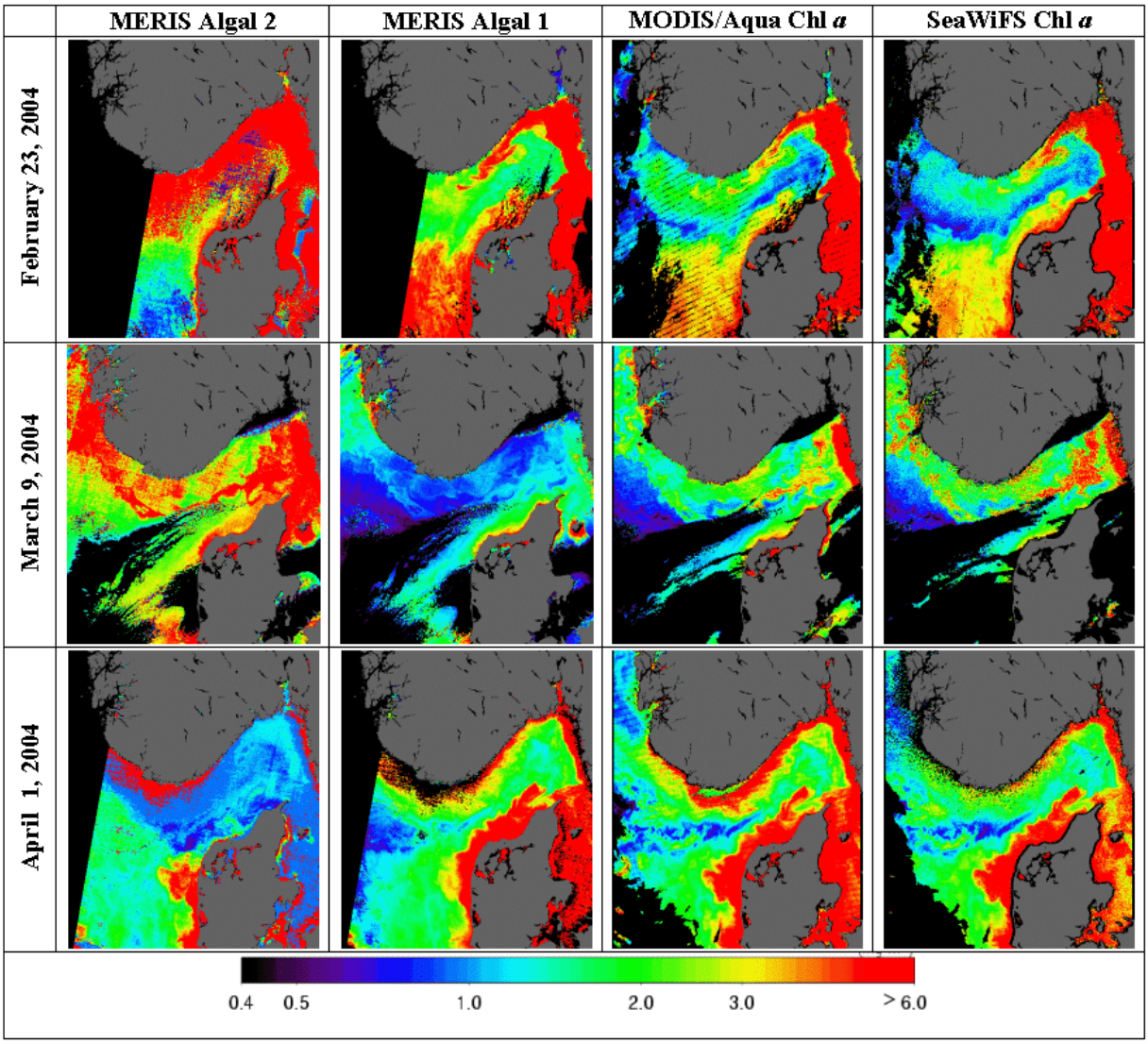

Figure 3: Chlorophyll distribution in North Sea and Skagerrak region as retrieved by the MERIS Algal 2, MERIS Algal 1, MODIS/Aqua Chl *a*, and SeaWiFS Chl *a* products (from left to right) for February 23, March 9 and April 1, 2004 (from top to bottom). Black areas indicate unprocessed pixels (clouds, corrupt atmospheric correction, or out of swath areas). Data are plotted with the same logarithmic colour scale, as indicated by the colour bar. The unit is $mg \cdot m^{-3}$. Copyright: ESA/NASA/Orbimage.

east of Lindesnes (the Southern-most point of Norway). All sensors seem to overestimate Chl *a* along the ferrybox transect (Table 3). However, compared to the Case 1 Chl *a* products in region A the overestimation is considerably less for MERIS Algal 2. In the SeaWiFS image pixelization or speckling is observed, as also reported and discussed by Hu *et al.* (2000) who state that pixelization is often due to digitization-noise errors in the bands at 765nm and 865nm used for the atmospheric correction. The error in Chl *a* due to this phenomenon is random but could be as high as ±65% (Hu *et al.* 2000), thus, Chl *a* can vary 2- to 3-fold between neighboring pixels. The MERIS Algal 1 data presented in this study, on the other hand, show less variability in retrieved Chl *a* values within neighboring pixels as compared to both MODIS/Aqua and SeaWiFS.

As already pointed out it has been shown that both the MODIS OC3M and SeaWiFS OC4v4 algorithms tend to overestimate Chl *a* in the southern North Sea (Blondeau-Patissier *et al.* 2004). This is obvious since these algorithms are tuned and validated for Case 1 waters. However, evaluations of the standard MODIS Case 2 water algorithm (Carder *et al.* 2003) in the same areas indicate no significant improvements as compared to the standard Case 1 water algorithm (Blondeau-

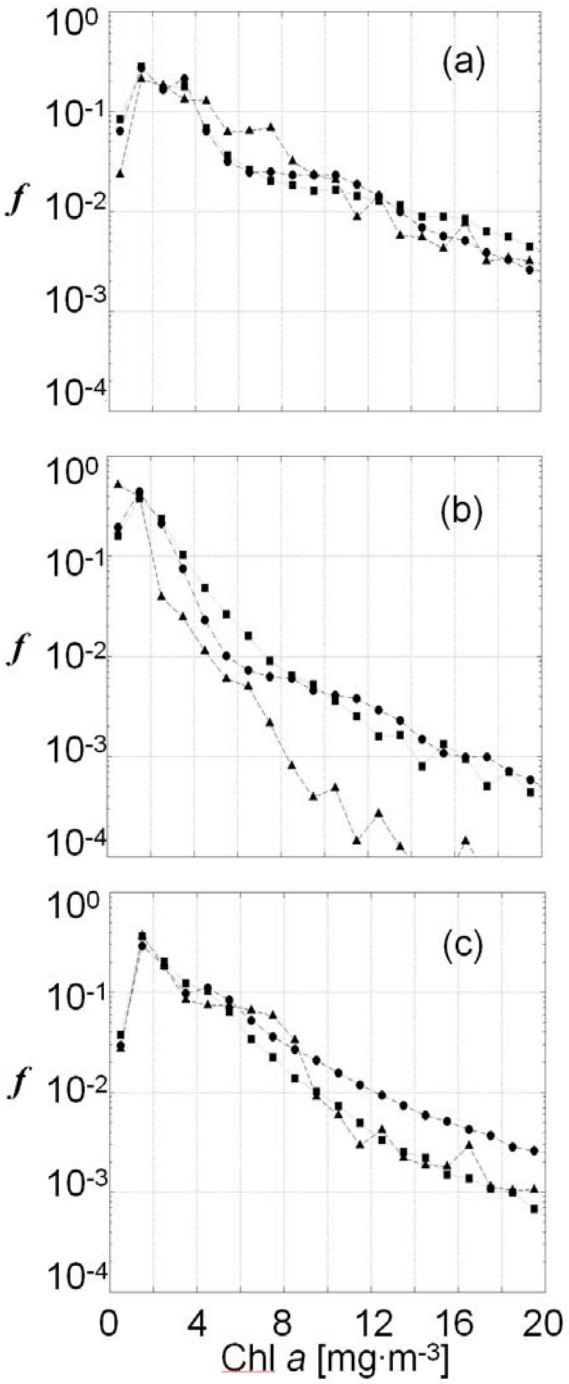

Figure 4: Frequency distribution of levels of retrieved chlorophyll *a* concentrations (Chl *a*) in sub-regions of the images shown in Fig. 3. Results are shown for MERIS Algal 1 (▲), MODIS/Aqua Chl *a* (●), and SeaWiFS Chl *a* (■), from February 23 (a), March 9 (b) and April 1 (c), 2004. Chl *a* is represented along the x-axis. The bin size is 1mg·m^{-3}, and the number of bins is 20, representing the concentration range 0-20mg·m^{-3}. The y-axis represents the fraction, *f*, of the number of pixels within each bin, n_b, to the total number of pixels in the image, n_{tot}, i.e. $f=n_b/n_{tot}$.

Patissier *et al.* 2004). Calibration and validation activities have further shown that the MERIS Case 2 water Algal 2 product is overestimating the Chl *a* in Skagerrak by a factor of 2 (Sørensen *et al.* 2003). In line with this, comparisons between satellite and ship borne data in this study (Table 3) show strong overestimation by the satellite products for two of the three dates (February 23 and March 30). However, underestimations are observed for the Case 1 Chl *a* products on March 9. The algorithms for Chl *a* retrievals in this area therefore still require tuning to local conditions. ESA has performed a MERIS data reprocessing (MERIS 2nd reprocessing, 2005) using an updated version of the Case 2 water algorithm for Chl *a* retrieval, which is considering local conditions based on ground truth observations (Sørensen, this issue). However, these reprocessed data were not available for evaluation in this study.

A major part of the study area is for all studied dates flagged as sediment-loaded Case 2 waters in the MERIS data products. Nevertheless, when evaluating the spatial distribution patterns of Chl *a* in the whole dataset, generally a better consistency between MERIS and the other sensors are found when applying the Algal 1 product, even though Algal 2 is observed to agree better in some areas for certain dates (e.g. in central Skagerrak on March 9 (Fig.2)). Furthermore, MERIS Algal 2 data acquired before March 26 occasionally depict Chl *a* values significantly higher than values retrieved by Case 1 water algorithms, and in some cases even unrealistically high as compared to expected algal bloom concentrations. For MERIS data after March 26, Algal 2 values are generally lower than Algal 1. However, from the results presented in Table 3, there are no indications that MERIS Algal 2 performs worse than the Case 1 water products as to retrieve reliable Chl *a* estimates as compared to the available *in situ* observations.

The MERIS data product suite also includes confidence and science L2 flags, as well as estimates of Total Suspended Matter (TSM), and Yellow Substance (YS). An evaluation of the quality of the Chl *a* products may be performed if the L2 flags, and the TSM and YS products are

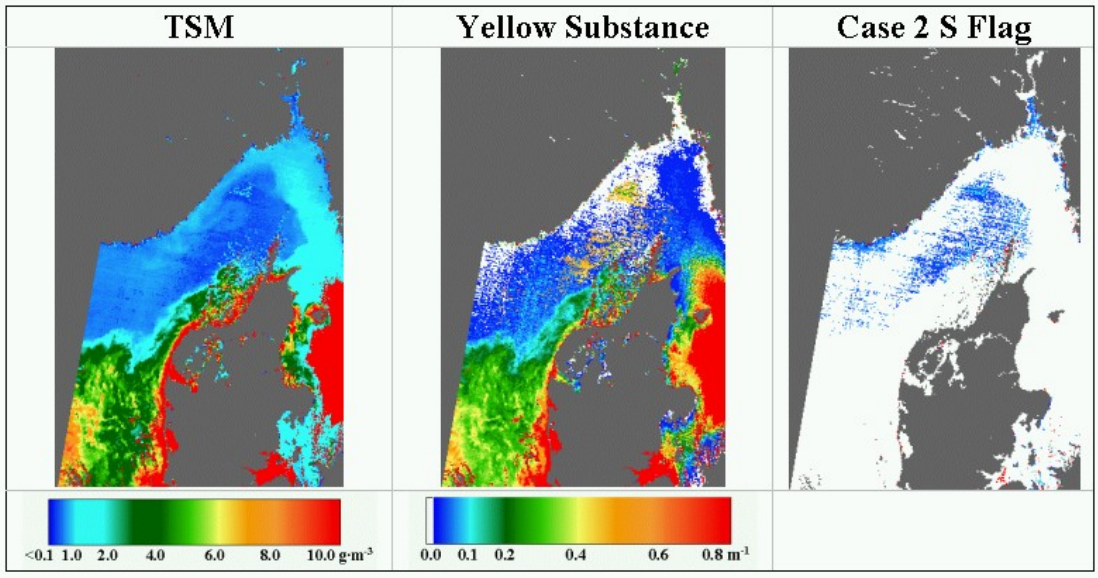

Figure 5: Concentrations of Total Suspended Matter (TSM) and Yellow Substance (YS) in Skagerrak retrieved by MERIS on February 23, 2004. In the image to the right white pixels indicate raising of the MERIS L2 science flag for sediment loaded Case 2 waters (Case 2 S).

interpreted in concert with the Chl *a* products (Fig. 5) Almost the entire area is flagged as sediment loaded Case 2 waters, indicating that the Algal 2 product should be valid, and Algal 1 consequently invalid. However, Algal 2 retrieves unrealistically high Chl *a* estimates as compared to Algal 1 in major parts of Skagerrak. As already shown (Table 3) for February 23 Algal 1 retrievals are much closer to ferrybox data in central Skagerrak, even though Algal 1 still overestimates Chl *a* by up to 167%. In the same region TSM and YS estimates are low, indicating that Algal 1 may be reliable even though the waters are flagged as Case 2. Furthermore, YS estimates are equal to zero (white colour) for some pixels, indicating algorithm failure. The overestimation of Chl *a* by Algal 2 may therefore be explained by the need of compensating for the (erroneously) low YS values. In the area west of Denmark, Algal 1 retrieves high Chl *a* values as well as high TSM and YS values. This indicates that the more moderate Algal 2 estimates may be more reliable for the area. Thus, it is shown that the MERIS Case 2 water flag alone may not be adequate for determining which of the two Chl *a* products should be trusted. However, TSM and YS estimates as well as available confidence and science L2 flags not investigated here may provide important information about the reliability of the Chl *a* products.

3.3 Comparison of Chl a in small areas

So far, the study has focused on comparison of the various sensor products and algorithms in connection with ferrybox data. However, in the following a relative inter-comparison is made between the *sensors*, rather than between the algorithms. To investigate sensor differences, the most important is to apply algorithms that are similar for all three sensors, given their different spectral band specifications (Table 2). The objective of the following analyses is therefore not to decide which of the sensors or algorithms that generates the most reliable product but rather to detect when the sensors perform similar and not.

The spatially averaged Chl *a* values for the seven small areas (Fig. 2) were compared for the three sensors (Fig. 6, Table 4). The MERIS Algal 2 values were also compared to the Case 1 water products fromall three sensors. However, the use of this product decreases the correlation and spatial consistency between MERIS and the other two sensors. Essentially no correlation was found between the MERIS Algal 2 product and respectively the MODIS/Aqua and SeaWiFS Chl *a* products. This observation is in line with the presumption that the Case 1 Chl *a* algorithms are

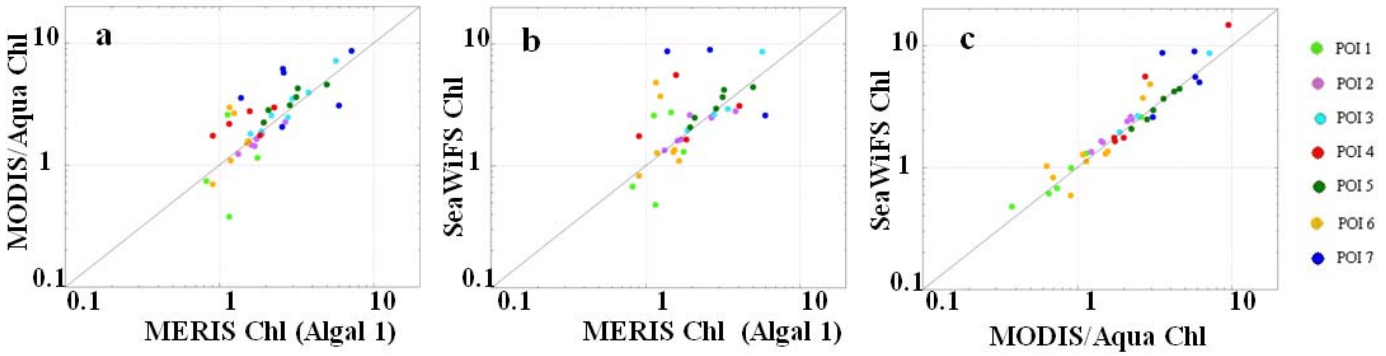

Figure 6: Scatter plots of averaged Chl *a* values within small areas (25 pixels) (see Fig. 2). Results are shown for MODIS/Aqua versus MERIS (a), SeaWiFS versus MERIS (b), and SeaWiFS versus MODIS/Aqua (c).

designed very similarly for the three sensors. In order to reach the goal of applying similar algorithms, only the Case 1 Chl *a* products are accordingly compared in the following. The better correlation was found between the MODIS/Aqua and SeaWiFS Chl *a* products (Table 4), with a coefficient of determination, r^2=0.82. The correlation between MERIS and MODIS/Aqua data was significantly less (r^2=0.60). No significant correlation was found between MERIS and SeaWiFS data (r^2=0.15). However, it was observed that the data discrepancies were mainly caused by results from 2-3 of the selected seven locations. Especially the data from Northern Skagerrak (location #7) showed no significant correlation between any of the three sensors. This may be due to the fact that this area is often loaded with yellow substance (YS) both from river discharges and from the Baltic water outflow. Furthermore, locations in North Sea water and in Central Skagerrak (respectively location #1 and #6) also contributed to reduce the overall correlations between the three EO data products. By excluding data from inner Skagerrak the correlation between the sensors improved significantly, see Table 4. The most optimal would be to compare sensors for pixels where the viewing angle is similar. However, due to different swath configurations this criterion is difficult to fulfil, at least in order to obtain a decent number of observations. As a consequence, different viewing angles may contribute to the observed discrepancy between sensors.

The MERIS Case 2 water flags were used to determine whether the locations for sensor inter-comparison were Case 1 or Case 2 waters. In

Table 4: The coefficient of determination, r^2, for the data presented in Figs 6 and 7 are shown. For the large (homogeneous) areas correlation is shown for the entire data range (0-12mgm^{-3}), for the low concentration range (0-2mgm^{-3}) and high concentration range (2-12mgm^{-3}). For the small areas correlation is shown for datasets with and without the inclusion of data from inner Skagerrak (#7).

	Large homogenous areas						Small fixed areas			
	All		Low		High		#1-7		#1-6	
Sensors compared	N	r^2	N	r^2	N	r^2	N	r^2	N	R^2
MER Algal 1-MOD/Aqua	28	0.92	19	0.91	9	0.75	41	0.60	35	0.76
MER Algal 1-SeaWiFS	28	0.93	19	0.88	9	0.81	35	0.15	32	0.44
MOD/Aqua–SeaWiFS	28	0.99	19	0.97	9	0.98	40	0.82	35	0.91
MER Algal 2-MER Algal 1							59	0.19		
MER Algal 2-MOD/Aqua							41	0.36		
MER Algal 2-SeaWiFS							35	0.20		

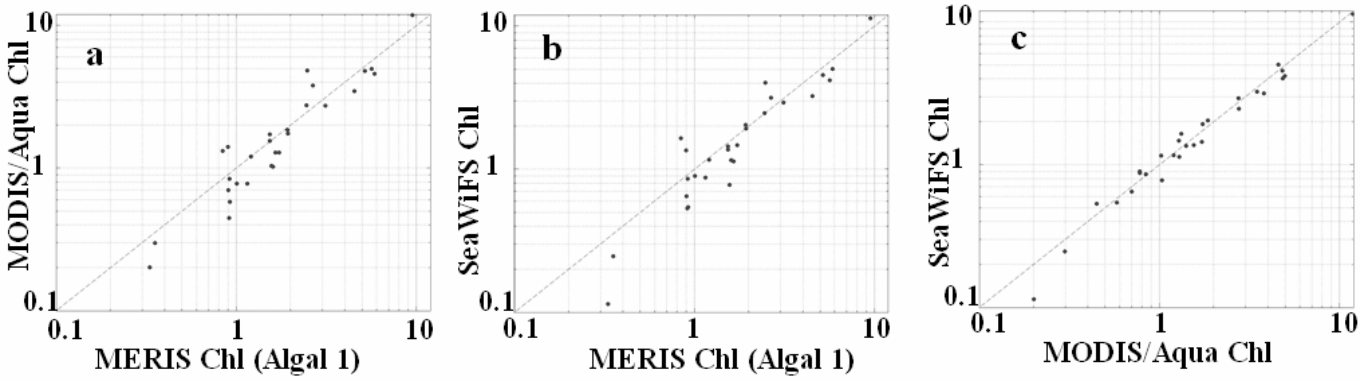

Figure 7: Scatter plots of averaged Chl *a* values within a total of 28 large homogeneous areas selected from the studied dataset (Table 1). Results are shown for MODIS/Aqua versus MERIS (a), SeaWiFS versus MERIS (b), and SeaWiFS versus MODIS/Aqua (c).

the statistical correlation analysis performed, it was not made a distinction between data locations categorized as Case 1 and Case 2 waters, since the overall results showed no significant changes in the correlation when the analysis was restricted to Case 1 or Case 2 water locations only.

3.4 Comparison of Chl a in large areas

The consistency between standard Chl *a* products from the three sensors was further evaluated by comparing the averaged values from 28 subjectively selected large (homogeneous) areas, as defined in section 2.4. Scatter plots of averaged values of Chl *a* derived from pairs of sensors are shown (Fig. 7), as well as the coefficients of determination, r^2 (Table 4). The correlation is shown for the entire dataset, as well as for respectively high (defined as Chl *a* > 2mg·m^{-3}) and low (Chl *a* < 2mg·m^{-3}) concentration ranges, representing typically algal bloom and non-bloom areas. The agreement between MODIS/Aqua and SeaWiFS data is very good (r^2=0.99) with no significant difference between low and high Chl *a* concentration ranges. The correlation between MERIS and MODIS/Aqua (r^2=0.92), and between MERIS and SeaWiFS (r^2=0.93) are slightly lower than between the two US sensors. The difference between MERIS and the two other sensors are most significant in the higher Chl *a* range. However, there is no trend in these data that shows a relative systematic over or under estimation of Chl *a* in either SeaWiFS or MODIS/Aqua data as compared to MERIS.

Considering sensor comparison for both the smalle areas (section 3.3) and for the large areas (above), the fact that the best correlation is found between MODIS/Aqua and SeaWiFS may be explained by several factors: (1) The algorithms for atmospheric correction and for the retrieval of Chl *a* are similar for the two sensors, i.e. the algorithm originally designed for SeaWiFS (O'Reilly *et al.* 1998) has only been modified to handle the MODIS band specifications (O'Reilly *et al.* 2000), and (2) the time difference between local overpass of the MODIS/Aqua and SeaWiFS sensors are less than between MERIS and the other two sensors. The maximum observed time gap between MODIS/Aqua and SeaWiFS was 1.5h, while it was 2.8h between MODIS/Aqua and MERIS, and 3.5h between MERIS and SeaWiFS (see Table 1). A temporal change in the measured ocean parameters may take place in between the overpass of the three different satellites, both due to time evolution and diurnal cycles. However, the effect of the time gap is considered to be small compared to algorithm differences between MERIS and SeaWiFS/MODIS when the data considered are averaged over large areas and obvious strong gradient areas are avoided. Thus, horizontal advection of the water masses during the time between the different satellite overpasses should not contribute significantly to the observed differences between the sensors when comparing the large areas. The similarity between MODIS and SeaWiFS has also been documented by Franz *et al.* (2005). When the same calibration techniques and atmospheric correction schemes are applied to the two sensors, they show that the resulting nLw products are in agreement to 5% on

the global average. More details and results of MODIS and SeaWiFS comparison are described by Feldman and McClain (2005a).

Several factors can explain why the agreement between the sensors was not as good for the small areas analysis as for the individually selected large areas. First of all the number of pixels averaged is much less than for the large areas, and high variations between neighbouring pixels would then introduce more noise in the dataset. Furthermore, the small areas were not pre-selected to represent homogenous areas, in contrast to the criterion for selecting the large areas. Therefore dynamic oceanic and atmospheric effects that could cause naturally induced differences are more likely to influence the results for the small areas. Such effects could include the advection of high Chl *a* gradients due to hydrodynamics, changing atmospheric conditions, and diurnal variations in the light conditions which could cause high temporal variability for the small areas, especially on a time scale of 2-3 hours. As already pointed out, different viewing geometry for each sensor may reduce the observed correlation between the sensor products. However, variations in viewing angles were not systematically checked for any of the comparison methods. This effect should therefore be equally important when comparing both the small and the large areas. But given the high correlation observed in the analysis for the large areas, it is not believed that variations in the viewing angle influence the analyses significantly in this case, and thus not for the case of the small areas either.

Considering only the Case 1 water products from the three sensors the observed discrepancies between the retrieved Chl *a* for large areas (~100 pixels) are assessed to be mainly due to inherent sensor and algorithm differences. However, the correlation between the Chl *a* products from all sensors is acceptable for practical use of the data in an NRT system for algal bloom monitoring. On the other hand, the increased discrepancy between the sensors when comparing the small areas (25 pixels) is probably due to temporal variability as well as the high variability between neighbouring pixels.

3.5 Evaluation and comparison of the atmospheric correction

The water-leaving reflectance and radiance spectra were analyzed for seven locations in the April 1 image. The physical conditions of the selected locations ranged from near-shore highly dynamic water masses to open ocean waters, and the phytoplankton conditions ranged from low to high Chl *a*. The normalized water-leaving radiance (nLw) is provided by both MODIS/Aqua and SeaWiFS and spectra of nLw were therefore directly compared between the two sensors. For offshore locations (more than 10 kilometres away from the coastline) the two US sensors retrieved almost identical radiance spectra. Significant differences in the spectra were only observed for two locations very close to land along the Norwegian coast in Skagerrak. However, for both MODIS/Aqua and SeaWiFS positive values of nLw in the shortest wavelength band (412nm) were only retrieved for one of the seven locations, confirming the deficiencies of the atmospheric correction algorithm (Siegel *et al.* 2000). In contrast, MERIS retrieved positive values of surface reflectance in all bands for six of the seven locations. Negative values in the blue spectral range were only observed for one station close to land.

It is a well-known fact that the atmospheric correction scheme for SeaWiFS often leads to an overcorrection in the blue when the radiance values are low (e.g. Siegel *et al.* 2000). Since the same atmospheric correction scheme is used for the processing of MODIS/Aqua, the fact that the two sensors' spectra show good agreement (even for negative values) is as expected. The MERIS atmospheric correction looks more robust in the sense that it retrieves physically valid (positive) values for almost all conditions. However, *in situ* validation of the surface reflectance for this region has shown an overestimation of 40% in the blue spectral range for the MERIS data (Sørensen *et al.* 2003). On the other hand, Gower and Borstad (2004) have shown that the signal-to-noise ratio of the 412nm band is about two or three times higher for MERIS than for MODIS and SeaWiFS, respectively. The algorithms for retrieval of Chl *a* in Case 1 waters are not for any of the three

sensors directly dependent on the spectral values retrieved in the blue band at 412nm. However, spectra with negative values in the blue indicate questionable atmospheric correction which may also influence the accuracy of the other spectral bands used for retrieval of Chl *a*.

4. Conclusions

A comparison of the capability to detect (H)ABs for the three ocean colour sensors MERIS, MODIS/Aqua, and SeaWiFS with regards to their respective Case 1 water Chl *a* products, and the normalized water-leaving radiance (MODIS and SeaWiFS) and the surface reflectance (MERIS) has been undertaken. The study shows a high level of correlation in the retrieved information between all sensors with regards to the Case 1 water Chl *a* products. The better correlation is found between the MODIS/Aqua and SeaWiFS sensors, which is obvious since the atmospheric correction schemes as well as the Chl *a* retrieval algorithms are based on similar conditions for these two sensors. Also, the difference in overpass time between MODIS/Aqua and SeaWiFS is generally less than between MERIS and any of the two US sensors. Further, the agreement between Chl *a* products for each pair of sensors depends on the method of comparison. The better correlation is found for data averaged over large areas (~100-1000 pixels) pre-selected to depict homogeneous values of Chl *a*, as compared to data averaged over small areas (25 pixels) that were not pre-selected as being homogeneous. The discrepancies between sensors when comparing large areas are assessed to be mostly due to inherent sensor and algorithm differences, while for small areas the discrepancies can also be explained by temporal variability in observation conditions as well as the high variability between neighbouring pixels.

The normalized water-leaving radiances (nLw) obtained by MODIS/Aqua and SeaWiFS show generally very good correspondence. In this analysis we did not convert values of nLw to surface reflectance as provided by MERIS. Hence, a direct comparison between the three sensors was not performed for these products. However, for six out of seven selected locations MERIS retrieved positive values of surface reflectance in the 412nm spectral band, while MODIS/Aqua and SeaWiFS retrieved positive values of nLw in this band for one location only. Values in the 412nm band do not directly influence the Chl *a* product for any of the sensors, but negative (physically unrealistic) values in this band indicate questionable values also in the bands used for calculation of Chl *a*. The algorithms for retrieval of Chl *a* in Case 1 waters are not for any of the three sensors directly dependent on the spectral values retrieved in the blue band at 412nm. However, spectra with negative values in the blue indicate questionable atmospheric correction which may also influence the accuracy of the other spectral bands used for retrieval of Chl *a*. This study shows no significant correlation between the MERIS Case 2 water Chl *a* product and the Case 1 water Chl *a* products from any of the three sensors, when comparing averaged data over the small areas. Comparisons between the MERIS Case 2 water Chl *a* product, all sensors' Case 1 water Chl *a* products, and *in situ* Chl *a* measurements were performed. These comparisons do not give a clear conclusion as to which Chl *a* product is the more reliable.

For a near real time algal bloom detection and monitoring system to be functional with a daily updated analysis of the phytoplankton situation, satellite data needs to be available in near real time, hence an integrated source of EO and *in situ* data is required. For the user of such services it should be transparent whether the satellite data originates from one or another sensor system. In order to obtain such consistency inter-calibration and product assessment between similar EO sensors such as MERIS, SeaWiFS, and MODIS need to be done on a regular basis throughout the life time of each mission. This is also a prerequisite for continued long time series used in monitoring of long-term trends and changes of inter-annual to decadal scales.

The observed similarity between MERIS and SeaWiFS in this study indicates that a replacement of SeaWiFS by MERIS data in the operational monitoring system does not introduce significant changes to the information flow of the monitoring system. However, using only the Case 1 water Chl *a* product from the MERIS sensor, the weaknesses observed with the equivalent

SeaWiFS product (regarding e.g. overestimation) will consequently persist. On the other hand this study also demonstrates that interpreting additional available MERIS products (e.g. TSM, YS, L2 science and confidence flags) in concert with Chl *a* for both Case 1 and 2 waters possibly improves the overall understanding of the atmospheric and marine conditions at the time of data acquisition. Thus, using this additional information an assessment of the reliability of the Chl *a* products can be performed. Moreover, with the recent MERIS reprocessing performed by ESA, improved quality of the data products relevant for the algal bloom detection and monitoring system is expected.

5. Acknowledgements

This work was performed through the project Integrating Modelling and Remote Sensing for Algae Bloom Monitoring in the Norwegian Waters (MORAN, #146155/S40) funded by the Research Council of Norway, the project Harmful Algal Bloom Initiation and Prediction in Large European Ecosystems (EVK3-CT-2001-00063 HABILE) funded by EC, and the project Data Integration System for Marine Pollution and Water Quality (DISMAR) (IST-2001-37657). The MERIS data have been provided through the ESA Envisat AO project number 813. The authors want to thank Kai Sørensen at Norwegian Institute for Water Research (NIVA) in Oslo, Norway, for his helpful input and comments. He kindly made available shipborne *in situ* Chl *a* measurements that were collected within the projects FerryBox (EVK2-CT-2002-00144), http://www.ferrybox.no and DISMAR.

References

AIKEN, J. and MOORE, G., 2000, Case 2 (S) Bright Pixel Atmospheric Correction. *MERIS ATBD 2.6* (Plymouth, UK: Plymouth Marine Laboratory).

ACKER, J. G., 1994, The heritage of SeaWiFS: A retrospective on the CZCS NIMBUS Experiment Team (NET) Program. *In SeaWiFS Technical Report Series*, NASA TM 1994-104566, Vol. 21, edited by S. B. Hooker, and E. R. Firestone (Greenbelt, Maryland: NASA Goddard Space Flight Center), pp. 1-44.

ANTOINE, D., and MOREL, A., 1999, A multiple scattering algorithm for atmospheric correction of remotely sensed ocean colour (MERIS instrument): principle and implementation for atmospheres carrying various aerosols including absorbing ones. *International Journal of Remote Sensing*, **20**, 1875-1916.

ANTOINE, D., and MOREL, A., 2000, Atmospheric Correction over the Ocean (Case 1 waters). *MERIS ATBD 2.7* (Laboratoire de Physique et Chimie Marines, France).

BARNES, R., CLARK, D., ESAIAS, W., FARGION, G., FELDMAN, G., and MCCLAIN, C., 2003, Development of a consistent multi-sensor global ocean colour time series. *International Journal of Remote Sensing*, **24**, 4047-4064.

BERGE, G. and FØYN, L. (editors), 1988, *Chrysocromulina polylepis* report: Rapport om oppblomstringen av Chrysocromulina polylepis i mai-juni 1988. Overvåkning, varsling og oppfølgende tiltak. Institute of Marine Research, Bergen.

BLONDEAU-PATISSIER, D., TILSTONE, G., MARTINEZ-VICENTE, V., and MOORE, G., 2004, Comparison of bio-physical marine products from SeaWiFS, MODIS and a bio-optical model with in situ measurements from Northern European waters. *Journal of Optics A-Pure and Applied Optics*, **6**, 875-889.

CARDER, K. L., CHEN, F. R., LEE, Z., HAWES, S. K., and CANNIZZARO, J. P., 2003, Case 2 Chlorophyll *a*. *MODIS Ocean Science Team Algorithm Theoretical Basis Document, ATBD 19,* version 7. (St. Petersburg., Florida, USA: College of Marine Science, University of South Florida,).

DARECKI, M., and STRAMSKI, D., 2004, An evaluation of MODIS and SeaWiFS bio-optical algorithms in the Baltic Sea. *Remote Sensing of Environment*, **89**, 326-350.

DOERFFER, R., SORENSEN, K., and AIKEN, J., 1999, MERIS potential for coastal zone applications. *International Journal of Remote Sensing*, **20**, 1809-1818.

DOERFFER, R., 2002, Protocols for the validation of MERIS water products. European Space Agency Doc. No. PO-TN-MEL-GS-0043.

DUNDAS, I., JOHANNESSEN, O. M., BERGE, G. and HEIMDAL, B. R., 1989. Toxic Algal Bloom in

Scandinavian Waters, May-June 1988. *Oceanography*, 2(1): 9-14.

DURAND, D., L.H. PETTERSSON, O.M. JOHANNESSEN, E. SVENDSEN, H. SØILAND and SKOGEN, M., 2002, Satellite observation and model prediction of toxic algae bloom. In *"Operational oceanography – Implementation at the European and regional scales"*. Editor in chief N.C. Flemming. Elsevier Oceanography Series Vol. 66, The Netherlands. ISBN 0 444 50391 9, pp. 505-515, 2002.

ESAIAS, W., ABBOTT, M., BARTON, I., BROWN, O., CAMPBELL, J., CARDER, K., CLARK, D., EVANS, R., HOGE, F., GORDON, H., BALCH, W., LETELIER, R., and MINNETT, P., 1998, An overview of MODIS capabilities for ocean science observations. *IEEE Transactions on Geoscience and Remote Sensing*, **36**, 1250-1265.

EVANS, R., and GORDON, H., 1994, Coastal Zone Color Scanner system calibration – a retrospective examination. *Journal of Geophysical Research –Oceans*, **99**(C4), 7293-7307.

FELDMAN, G. C., and MCCLAIN, C. R., 2005a, Ocean Color Validation, Ocean Color Web, Eds. KURING, N., BAILEY, S. W., THOMAS, D., FRANZ, B. F., MEISTER, G., WERDELL, P. J., EPLEE, R. E., MACDONALD, M., and RUBENS, M. 20 July 2005. NASA Goddard Space Flight Center. 29 August 2005. http://oceancolor.gsfc.nasa.gov/VALIDATION/

FELDMAN, G. C., and MCCLAIN, C. R., 2005b, MODISAqua Ocean Reprocessing 1.1, Ocean Color Web, Eds. KURING, N., BAILEY, S. W., THOMAS, D., FRANZ, B. F., MEISTER, G., WERDELL, P. J., EPLEE, R. E., MACDONALD, M., and RUBENS, M. 28 July 2005. NASA Goddard Space Flight Center. 29 August 2005. http://oceancolor.gsfc.nasa.gov/REPROCESSING/Aqua/R1.1/

FOURNIER-SICRE, V., and BELANGER, S., 2002, Intercomparison of SeaWiFS and MERIS marine products on Case 1 waters. *Proceedings of Envisat Validation Workshop, 9 – 13 December 2002 (ESA SP-531, August 2003)* (Frascati, Italy).

FRANZ, B., 2005, The Continuity of Ocean Color Measurements from SeaWiFS to MODIS, *SPIE Earth Observing Systems X*, July 31 - August 4, 2005.

GORDON, H. R., and WANG, M., 1994, Retrieval of water-leaving radiance and aerosol optical thickness over the oceans with SeaWiFS: a preliminary algorithm. *Applied Optics*, **33**, 443-452.

GOWER, J. and BORSTAD, G., 2004, On the potential of MODIS and MERIS for imaging chlorophyll fluorescence from space. *International Journal of Remote Sensing*, **25**, 1459-1464.

GREGG, W., ESAIAS, W., FELDMAN, G., FROUIN, R., HOOKER, S., MCCLAIN, C., and WOODWARD, R., 1998, Coverage opportunities for global ocean color in a multimission era. *IEEE Transactions on Geoscience and Remote Sensing*, **36**, 1620-1627.

HOOKER, S. B., ESAIAS, W. E., FELDMAN, G. C., GREGG, W. W., and MCCLAIN, C. R., 1992, An Overview of SeaWiFS and Ocean Color. *In SeaWiFS Technical Report Series*, NASA TM 1992-104566, Vol. 1, edited by S. B. Hooker and E. R. Firestone (Greenbelt, Maryland: NASA Goddard Space Flight Center), pp. 1-24 with 5 colour plates.

HORSTMANN, U., LU, D., GÖBEL, J., DAVIDOF, A., DAHL, E. and KAAS, H., 1998, Tracing a toxic algal bloom of *Chattonella* around the southern Norway and West Jutland, using MOS and SeaWiFS satellite data. *2nd International Workshop on MOS-IRS and Ocean Colour*, Wissenschaft und Technik Verl., Berlin, 1998, 303-311.

HU, C., CARDER, K., and MULLER-KARGER, F., 2000, How precise are SeaWiFS ocean color estimates? Implications of digitization-noise errors. *Remote Sensing of Environment*, **76**, 239-249.

JOHANNESSEN, O.M., OLAUSSEN, T. I., PETTERSSON, L. H., JOHANNESSEN, J. A., HAUGAN, P. M., KLOSTER, K., SANDVEN, S., HANSEN, L, and GEIGER, C., 1989, The Toxic Algal Bloom in May 1988, with recommendations for future application of remote sensing. *NRSC Special Report No. 1*, for the Norwegian Space Centre.

KWIATKOWSKA, E., and FARGION, G., 2003, Application of machine-learning techniques

toward the creation of a consistent and calibrated global chlorophyll concentration baseline dataset using remotely sensed ocean color data. *IEEE Transactions on Geoscience and Remote Sensing*, **41**(12), 2844-2860.

LEE, Z., and CARDER, K., 2002, Effect of spectral band numbers on the retrieval of water column and bottom properties from ocean color data. *Applied Optics*, **41**, 2191-2201.

MERIS Quality Working Group, 2005, MERIS 2nd reprocessing: Changes description. 01/08/2005 –Version 1.

MOORE, G., AIKEN, J., and LAVENDER, S. J., 1999, The atmospheric correction of water colour and the quantitative retrieval of suspended particulate matter in Case II waters: application to MERIS. *International Journal of Remote Sensing*, **20**(9), 1713-1733.

MOREL, A. and ANTOINE, D., 2000, Pigment Index Retrieval in Case 1 Waters. *MERIS ATBD 2.9* (France: Laboratorie de Physique et Chimie Marines).

O'REILLY, J., MARITORENA, S., MITCHELL, B., SIEGEL, D., CARDER, K., GARVER, S., KAHRU, M., and MCCLAIN, C., 1998, Ocean color chlorophyll algorithms for SeaWiFS. *Journal of Geophysical Research -Oceans*, **103**, 24937-24953.

O'REILLY, J. E., MARITORENA, S., SIEGEL, D., O'BRIEN, M. C., TOOLE, D., MITCHELL, B. G., KAHRU, M., CHAVEZ, F. P., STRUTTON, P., COTA, G., HOOKER, S. B., MCCLAIN, C. R., CARDER, K. L., MULLER-KARGER, F., HARDING, L., MAGNUSON, A., PHINNEY, D., MOORE, G. F., AIKEN, J., ARRIGO, K. R., LETELIER, R., and CULVER, M., 2000, Ocean color chlorophyll a algorithms for SeaWiFS, OC2, and OC4: Version 4. *In SeaWiFS Postlaunch Technical Report Series*, Vol. 11, edited by S. B. Hooker, and E. R. Firestone (Greenbelt, Maryland, USA: NASA Goddard Space Flight Center), pp. 9-23.

PETTERSSON, L. H., DURAND, D., SVENDSEN, E., and SØILAND, H., 2000, DeciDe for near real-time use of ocean colour data in management of harmful algae blooms. Satellite EO monitoring of the harmful algae bloom of Chattonella in the North Sea in April-May 2000. *NERSC Technical Report no. 199*, (Bergen, Norway: Nansen Environmental and Remote Sensing Center), pp. 34.

PETTERSSON, L. H., ALLAN, J. I., ANDERSEN, P., FIGUERAS, F. G., GROOM, S., KAITALA, S., KARLSON, B., LORENTZEN, T., MILLER, P., NAUSTVOLL, L. J., NEUMANN, A., SKOGEN, M., STIPA, T., SVENDSEN E., and TORRES, R., 2005, Final scientific report under Harmful Algal Bloom Initiation and Prediction in Large European Marine Ecosystems – HABILE, EC FP5 contract EVK3-CT2001-00063. *NERSC technical report no. 259*, February 2005.

RAST, M., BEZY, J., and BRUZZI, S., 1999, The ESA Medium Resolution Imaging Spectrometer MERIS - a review of the instrument and its mission. *International Journal of Remote Sensing*, **20**, 1681-1702.

SIEGEL, D., WANG, M., MARITORENA, S., and ROBINSON, W., 2000, Atmospheric correction of satellite ocean color imagery: the black pixel assumption. *Applied Optics*, **39**, 3582-3591.

SÆTHRE, R., and MORK, M., 1981, The Norwegian Coastal Current. *University of Bergen press.*

SØRENSEN, K., AAS, E., HØKEDAL, J., SEVERINSEN, G., DOERFFER, R., and DAHL, E., 2003 Validation of MERIS water products in the Skagerrak. *Proceedings from Envisat MAVT-2003 - Working meeting on MERIS and AATSR Calibration and Geophysical Validation.*

ZIBORDI, G., MELIN, F., HOOKER, S., D'ALIMONTE, D., and HOLBERT, B., 2004, An autonomous above-water system for the validation of ocean color radiance data. *IEEE Transactions on Geoscience and Remote Sensing*, **42**, 401-415.